

## SYNTHESIS OF COBALT FERRITE NANOPARTICLES USING MICROEMULSION METHOD: STRUCTURE, MORPHOLOGY, AND MAGNETIC PROPERTIES

M. Bodiul Islam<sup>1\*</sup>, M. Rahat Pavel<sup>1</sup>, M. Rafizul Islam<sup>1</sup> and M. Jahidul Haque<sup>1</sup>

<sup>1</sup>Department of Glass & Ceramic Engineering, Rajshahi University of Engineering & Technology (RUET), Rajshahi-6204, Bangladesh

Received: 11 March 2022

Accepted: 14 June 2022

### ABSTRACT

Cobalt ferrite nanoparticles were prepared by the microemulsion method. Different values of pH of the microemulsion were maintained to find out the optimum pH to prepare cobalt ferrite nanoparticles. Prepared nanoparticles were characterized using X-ray Powder Diffraction (XRD), Vibrating Sample Magnetometer (VSM), and Scanning Electron Microscope (SEM). Rietveld refinement was used to analyze the crystal structure of the prepared cobalt ferrite nanoparticles. The crystallite size of prepared nanoparticles has been found from XRD in the range of 13.79 nm to 30.40 nm. The saturation magnetization, remanent magnetization, and coercivity have been found to be 12.05 emu/g, 0.77 emu/g, and 118.912 Oe respectively from VSM measurements.

**Keywords:** Cobalt ferrite nanoparticles, Rietveld refinement, Scanning Electron Microscope (SEM), Vibrating Sample Magnetometer (VSM), and X-ray Powder Diffraction (XRD).

### 1. INTRODUCTION

Nanotechnology deals with the fabrication, study, and applications of materials with at least one dimension of 1 to 100 nm. The unique physical and chemical properties of nanomaterials are strongly related to their size and exhibit novel properties compared with their bulk counterparts having similar chemical composition. The ratio of the number of surface atoms to bulk atoms increases with decreasing the size of nanomaterials and introduces significant changes in properties (Mathew & Juang, 2007; Méndez-Vilas, 2013). Magnetic nanoparticles are being extensively studied due to their strong sensitivity to the applied magnetic field and the capability to get functionalized and/or encapsulated with drug molecules (Agnieszka Z. Wilczewska, Katarzyna Niemirowicz, Karolina H. Markiewicz, 2012; Bamrungsap et al., 2012; H. Maeda, J. Wu, T. Sawa, Y. Matsumura, 2000; Patra et al., 2018; Yu et al., 2015). Applications of Magnetic nanoparticles include but are not limited to the data storage systems, magnetic fluids, catalysis, and bioapplications like detection of biological entities, magnetic bioseparation, clinic diagnosis and therapy (such as magnetic resonance imaging (MRI) and hyperthermia), targeted and controlled drug delivery, and biological labels (Foroughi et al., 2015; Mathew & Juang, 2007; Wu et al., 2008). Among different types of magnetic nanoparticles, biocompatible iron oxide nanoparticles have received considerable attention for their potential applications as an enhancing agent in MRI, active agent in drug delivery, tissue repair, cell separation, etc. (Angelique Y. Louie, Martina M. Hüber, Eric T. Ahrens, Ute Rothbächer, Rex Moats, Russell E. Jacobs, Scott E. Fraser, 2000; Gupta & Gupta, 2005; Jun et al., 2005; Mohapatra et al., 2011; Perez et al., 2004; Wu et al., 2008). However, due to their high chemical activity, the bare iron oxide nanoparticles are easily oxidized in air, resulting in loss of magnetism and dispersibility (Wu et al., 2008). Furthermore, the low coercivities of pure iron oxides restrict their applications in the high-density recording. Modification with cobalt enhances the coercivities of iron oxides (Sharrock, 1989; V. Pillai, 1996). Spinel cobalt ferrite ( $\text{CoFe}_2\text{O}_4$ ) has high coercivity ( $H_c$ ) and moderate magnetization ( $M_s$ ) with immense physical and chemical stability, which make  $\text{CoFe}_2\text{O}_4$  nanoparticles suitable for high-density digital recording (Chinnasamy et al., 2003; Houshiar et al., 2014; Mohapatra et al., 2011; Shafi et al., 1998). Moreover, applications of cobalt ferrite nanoparticles in therapeutic applications add several benefits due to their large magnetic anisotropy (Cannas et al., 2006; Fortin et al., 2007; Mohapatra et al., 2011). In the lattice structure of cobalt ferrite, the octahedral sites are occupied by the  $\text{Co}^{2+}$  ions and half of the  $\text{Fe}^{3+}$  ions, while tetrahedral sites are occupied by the other half of the  $\text{Fe}^{3+}$  ions, which is a complete inverse spinel structure (Goldman, 2006; Verwey & Heilmann, 1947; Zeng et al., 2017).

The method of formation of cobalt ferrite nanoparticles has an effect on the size, size distribution, shape, and consequently on the final properties of the fabricated nanoparticles. Moreover, the change of properties is not regular. While the ferromagnetic  $\text{CoFe}_2\text{O}_4$  nanoparticles have prospect in permanent magnetic applications, the

\*Corresponding Author: [mbi@gce.ruet.ac.bd](mailto:mbi@gce.ruet.ac.bd)

<https://www2.kuet.ac.bd/JES/>

ISSN 2075-4914 (print); ISSN 2706-6835 (online)

superparamagnetic  $\text{CoFe}_2\text{O}_4$  nanoparticles have prospect in biomedical applications (Duong *et al.*, 2021). So, further research work on the fabrication method of cobalt ferrite nanoparticles is required. The available methods of fabricating cobalt ferrite nanoparticles are solid-state reaction (Khedr *et al.*, 2006), reverse micelles (Calero-DdelC & Rinaldi, 2007), chemical co-precipitation (Zi *et al.*, 2009), hydrothermal method (Chen *et al.*, 2009), sol-gel (Gul & Maqsood, 2008), combustion (Franco *et al.*, 2011), and microemulsion (A. Bee, R. Massart, 1995; Sinkó *et al.*, 2012), etc. Every method has its pros and cone. For example, the thermal decomposition method generates highly monodispersed particles with a narrow size distribution, but the fabricated nanoparticles are usually capable of dissolving only in nonpolar solvents. Co-precipitation method produces nanoparticles with a wide size distribution, consequently it needs particles separation process after fabrication (Wu *et al.*, 2008). Among the formation methods of cobalt ferrite nanoparticles, the microemulsion is a promising method due to the better control of shape and size of the nanoparticles, but, careful investigation is needed to find the effect of process parameters on the properties of nanoparticles. In this research report, the synthesis of the nanoparticles was done by the microemulsion method and the characterization of the nanoparticles was performed by XRD, SEM, and VSM. The Rietveld analysis was used to analyze the structure of the fabricated nanoparticles.

## 2. MEHODOLOGY

Beakers, measuring cylinder, glass rod, mortar pestle were washed and cleaned in an ultrasonic cleaner. After cleaning, the instruments were dried at 90 °C for several minutes in a dryer. Ferric chloride hexahydrate ( $\text{FeCl}_3 \cdot 6\text{H}_2\text{O}$ ), cobalt chloride hexahydrate ( $\text{CoCl}_2 \cdot 6\text{H}_2\text{O}$ ), and sodium hydroxide (NaOH) were weighed using electric balance up to two decimal numbers. Distilled water and oleic acid were measured using a measuring cylinder. 3.25 ml of 0.4 M iron chloride ( $\text{FeCl}_3 \cdot 6\text{H}_2\text{O}$ ) solution and 25 ml of 0.2 M cobalt chloride ( $\text{CoCl}_2 \cdot 6\text{H}_2\text{O}$ ) solution were taken in a beaker; distilled water was added to make the solution 100 ml followed by mixing thoroughly. Pellets of sodium hydroxide were crushed to smaller particles using a mortar pestle for quick dissolution. 2.3 M sodium hydroxide solution was made by mixing 9.6 gm of crushed sodium hydroxide pellets in 100 ml distilled water. Sodium hydroxide was added drop by drop to the solution maintaining continuous stirring to increase the pH and different pH level (12, 12.5, and 13) was tried to find out the optimum level of pH to prepare the nanoparticles (Figure 1). It is noteworthy that the nanoparticles were obtained at pH level 13.



**Figure 1:** Adjusting pH and the solution after adjusting pH.

Oleic acid (40 ml) was added as a surfactant and after that precipitation was found. The precipitated liquid was stirred continuously for 2 hrs at 85 °C and then the liquid was cooled slowly to room temperature. The solid precipitate was separated by filtration and the precipitate was washed with 1:1 ethanol and distilled water to remove impurities. Supernate was poured out and subsequently centrifuge operation for 20 min at 4500 rpm was applied to remove the remaining liquid with the particles.

Prepared black particles were dried in an oven at 120 °C for 24 hrs. After grounding into fine powders, the particles were annealed at 900 °C for 11 hrs maintaining a firing schedule (Figure 2). The temperature was increased from room temperature to 900 °C within 5 hrs. This temperature was held for 1 hr. Then the sample was cooled back to room temperature (25 °C) within 5 hrs.

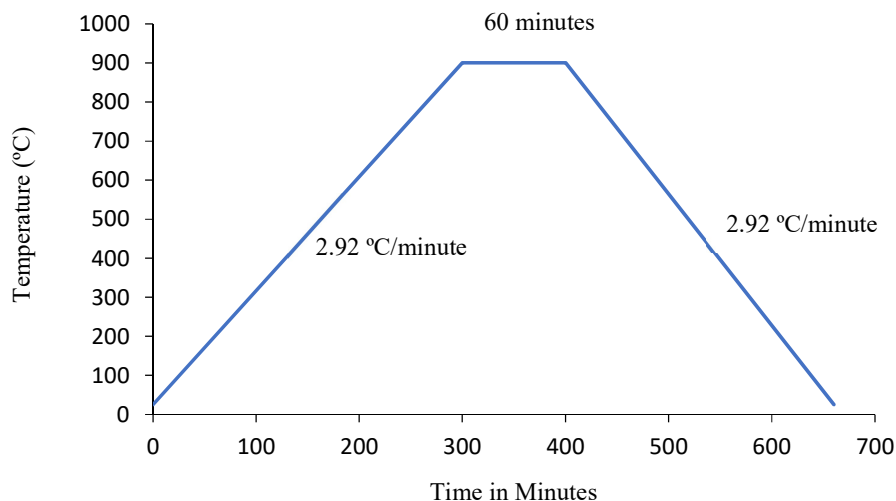


**Figure 2:** Firing Schedule of fabricating cobalt ferrite nanoparticles.

### 3. RESULTS AND DISCUSSION

#### 3.1 Structural Properties Analysis

The crystallographic structure of the powder was characterized by x-ray diffraction (XRD) and the XRD pattern shows that both the peaks of cobalt ferrite and cobalt chloride are present (Figure 3). The reasons for cobalt chloride inclusion may be the raw materials that didn't take part in the reaction. Improper nucleation may be the reason behind this phenomenon too. The diffraction peaks of (1 1 1), (2 2 0), (2 2 2), (3 1 1), (4 0 0), (4 1 1), (4 4 0) and (5 3 1) planes are corresponding to spinel cobalt ferrite. The average crystallite size was calculated from the XRD data using Scherer equation (Cullity, 1978). The crystallite size of prepared cobalt ferrite ranged from 13.79 nm to 30.40 nm and the second phase of cobalt chloride was from 13.44 nm to 42.72 nm.

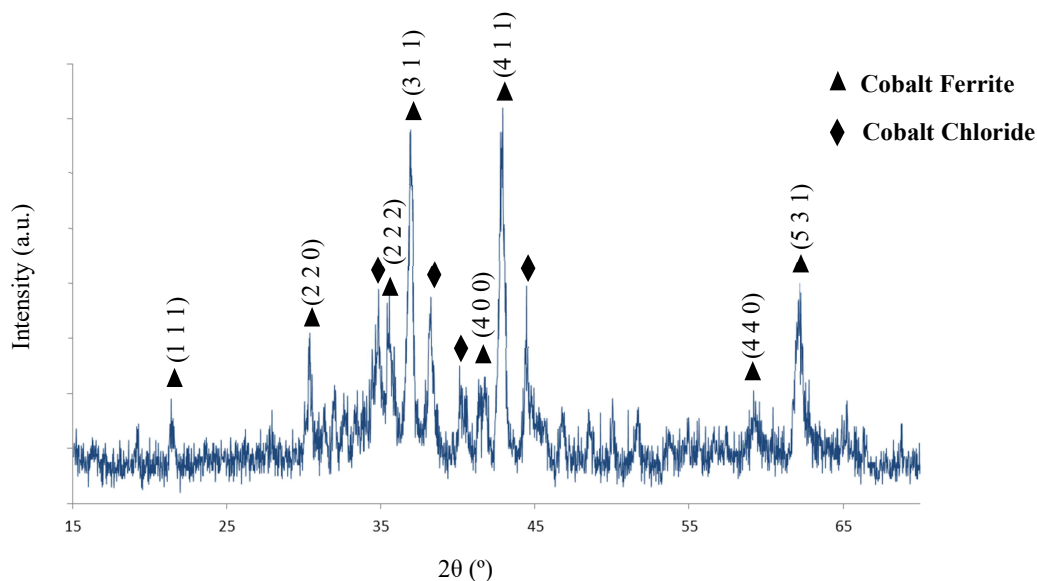


**Figure 3:** XRD pattern of prepared cobalt ferrite nanoparticles.

#### Rietveld Refinement

Rietveld refinement is a technique described by Hugo Rietveld to characterize the crystal structure of materials. Using a least-squares approach, this method processes a theoretical line to match the measured profile (M. R.

Gauna, M. S. Conconi, S. Gomez, G. Suarez, E. F. Aglietti, 2015; Rietveld, 1969). The following graph of intensity vs.  $2\theta$  shows the Rietveld refinement of the prepared cobalt ferrite nanoparticles (Figure 4).

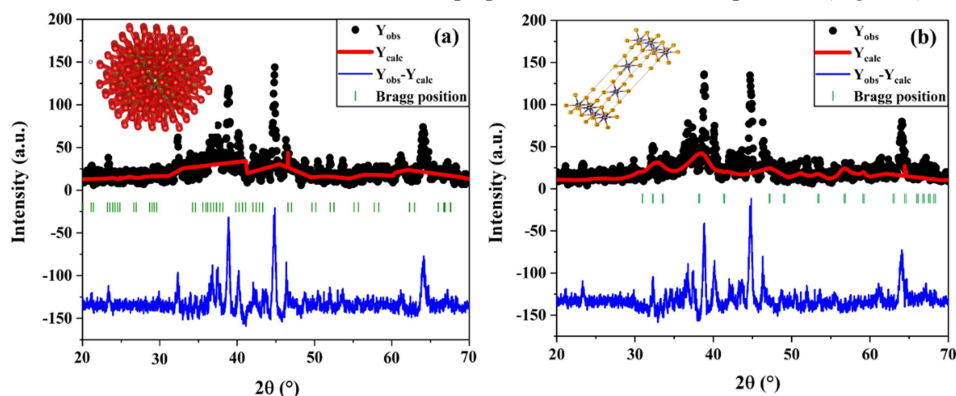


**Figure 4:** Rietveld Refinement of the XRD pattern for (a) cobalt ferrite and (b) cobalt chloride phases (Inset shows the crystal structure of the corresponding phases).

The black part of the curve indicates the prepared cobalt ferrite nanoparticles and the green part shows the standard Bragg position of corresponding phase (Figure 4 (a)). The red line expresses the mismatch between the prepared sample and the standard one. The reason behind this mismatch between the curves is the presence of unwanted phases like cobalt chloride which is shown in Figure 3. However, the Rietveld refined parameters of the XRD patterns are included in Table 1.

The bond length between necessary atoms was also measured in the Rietveld refinement process. The bond lengths measured here are, Fe-O = 2.45 Å, Co-O = 2.45 Å, O-O = 2.45 Å. The density of the prepared sample was 5.04 gm/cm<sup>3</sup>.

**Table 1:** Rietveld refinement of cobalt ferrite nanoparticles.

Composition	Space group	Lattice constants (Å)	Unit cell volume (Å <sup>3</sup> )	Reliability factors (%)	GoF	Bragg R Factor	RF Factors
Cobalt ferrite	<i>Fd-3m</i>	a = 2.80636 b = 2.80636 c = 2.80636	22.102	Rp = 37.2 Rwp = 43.3 Rexp = 21.3	2.2	92.2	72.6
Cobalt chloride	<i>R-3m</i>	a = 3.24408 b = 3.24408 c = 17.33810	158.021	Rp = 34.6 Rwp = 21.4 Rexp = 20.5	2.0	99.4	93.3

### 3.2 Magnetic Property Analysis

Room temperature magnetic properties of the cobalt ferrite were measured using a vibrating sample magnetometer (VSM). The saturation magnetization ( $M_s$ ), remnant magnetization ( $M_r$ ), and coercivity ( $H_C$ ) were determined from obtained hysteresis loops. Magnetization vs magnetic field (M-H) curve up to 10,000 Oe at room temperature shows the hysteresis loop and the loop forms S-shaped (Figure 5). The obtained S-shaped hysteresis loop is thinner compared to other works in literature in which cobalt ferrite nanoparticles were prepared in solid state and Solvothermal Processes (Duong *et al.*, 2021; Khedr *et al.*, 2006). This may happen due to the presence of cobalt chloride phase. Saturation magnetization is the maximum magnetization, after reaching it; magnetization does not increase with increasing magnetic field. The saturation magnetization ( $M_s$ ) of the sample is 12.05 emu/g. The upward part of the sample is 12.05 emu/g and the downward part is -12.05 emu/g. The value of  $M_s$  is smaller in nano-sized materials than the bulk material (Gu *et al.*, 2008). The required field to demagnetize the sample is known as the coercive field. From the hysteresis loop, we can see the coercive fields of the prepared sample are 136.09 Oe and -101.74 Oe. The average coercive field of the prepared cobalt ferrite nanoparticles sample is 118.92 Oe. The value of magnetization after removing the magnetic field is known as remanent. The downward part remanence of the sample is -0.91 emu/g and the upward part remanent of the sample is 0.63 emu/g. The average remanence magnetization of cobalt ferrite nanoparticles sample is 0.77 emu/g. It is clearly visible that the remanent of the prepared sample is very low. It

means that it is easy to magnetize and demagnetize the sample by applying an external field. These are the properties of soft ferrimagnetic materials.

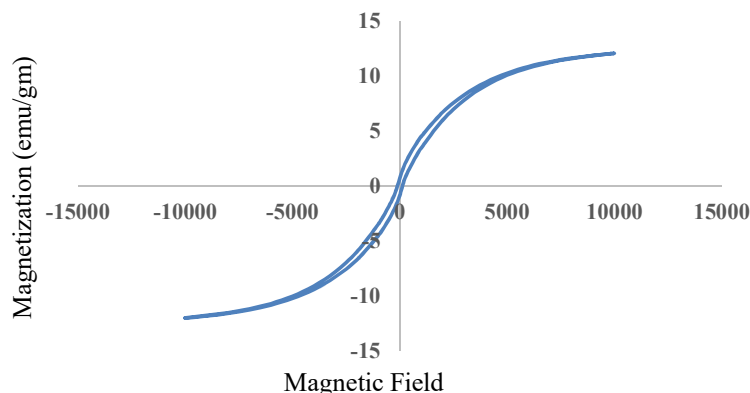


**Figure 5:** Magnetization curve at room temperature.

### 3.3 Morphological Analysis

To reveal the morphology of the fabricated cobalt ferrite nanoparticles, scanning electron microscope images were taken. The images of Figure 6 show particles with some agglomerations. The reason for agglomerations might be unwanted phases like cobalt chloride. This unwanted phase might be generated due to the unreacted raw materials.

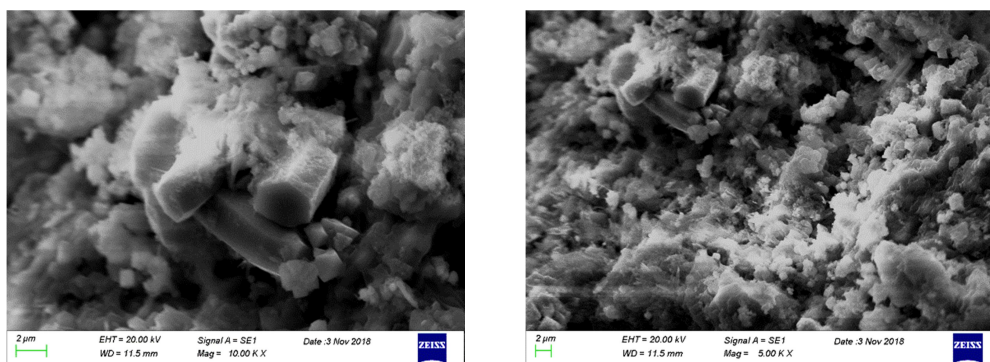


**Figure 6:** SEM images of  $\text{CoFe}_2\text{O}_4$  nanoparticles.

## 4. CONCLUSIONS

The synthesis of the cobalt ferrite nanoparticles was done by the microemulsion method. Different pH (12, 12.5, and 13) was maintained to prepare cobalt ferrite nanoparticles and the nanoparticles were prepared only at pH 13. The drying temperature was  $120^\circ\text{C}$  and the firing temperature was  $900^\circ\text{C}$ . The prepared cobalt ferrite nanoparticles were blackish in color and the crystal structure was inverse spinel. The crystallite size was between 13.79 nm and 30.40 nm. The hysteresis loop was S-shaped. The VSM result showed that average coercivity was 118.92 Oe, average remanent magnetization was 0.77 emu/g and average saturation magnetization was 12.05 emu/g. The remanent of the prepared particles was very low which indicates the property of ferrimagnetic material.

### Acknowledgements

The authors would like to thank the Rajshahi University of Engineering & Technology and Atomic Energy Center, Bangladesh, for their support during this research work.

### REFERENCES

- A. Bee, R. Massart, S. N. (1995). Synthesis of very fine maghemite particles. *Journal of Magnetism and Magnetic Materials*, 149, 6–9. [https://doi.org/SSDI 0304-8853\(95\)00317-7](https://doi.org/SSDI 0304-8853(95)00317-7)

- Agnieszka Z. Wilczewska, Katarzyna Niemirowicz, Karolina H. Markiewicz, H. C. (2012). Nanoparticles as drug delivery systems. *Pharmacological Reports*, 64, 1020–1037.
- Angelique Y. Louie, Martina M. Hüber, Eric T. Ahrens, Ute Rothbächer, Rex Moats, Russell E. Jacobs, Scott E. Fraser, M. T. J. (2000). In vivo visualization of gene expression using magnetic resonance imaging. *NATURE BIOTECHNOLOGY*, 18, 321–325.
- Bamrungsap, S., Zhao, Z., Chen, T., Wang, L., Li, C., Fu, T., & Tan, W. (2012). Nanotechnology in therapeutics: a focus on nanoparticles as a drug delivery system. *Nanomedicine*, 7(8), 1253–1271. <https://doi.org/10.2217/nnm.12.87>
- Calero-DdelC, V. L., & Rinaldi, C. (2007). Synthesis and magnetic characterization of cobalt-substituted ferrite (CoFe<sub>3-x</sub>O<sub>4</sub>) nanoparticles. *Journal of Magnetism and Magnetic Materials*, 314(1), 60–67. <https://doi.org/10.1016/j.jmmm.2006.12.030>
- Cannas, C., Musinu, A., Peddis, D., & Piccaluga, G. (2006). Synthesis and Characterization of CoFe<sub>2</sub>O<sub>4</sub> Nanoparticles Dispersed in a Silica Matrix by a Sol–Gel Autocombustion Method. *Chemistry of Materials*, 18(16), 3835–3842. <https://doi.org/10.1021/cm060650n>
- Chen, L., Shen, Y., & Bai, J. (2009). Large-scale synthesis of uniform spinel ferrite nanoparticles from hydrothermal decomposition of trinuclear heterometallic oxo-centered acetate clusters. *Materials Letters*, 63(12), 1099–1101. <https://doi.org/10.1016/j.matlet.2009.02.034>
- Chinnasamy, C., Senoue, M., Jeyadevan, B., Perales-Perez, O., Shinoda, K., & Tohji, K. (2003). Synthesis of size-controlled cobalt ferrite particles with high coercivity and squareness ratio. *Journal of Colloid and Interface Science*, 263(1), 80–83. [https://doi.org/10.1016/S0021-9797\(03\)00258-3](https://doi.org/10.1016/S0021-9797(03)00258-3)
- Cullity, B. D. (1978). *Elements of X-ray Diffraction* (2nd ed.). Addison-Wesley Publishing Co., Inc.
- Duong, H. D. T., Nguyen, D. T., & Kim, K. S. (2021). Effects of process variables on properties of CoFe<sub>2</sub>O<sub>4</sub> nanoparticles prepared by solvothermal process. *Nanomaterials*, 11(11), 1–17. <https://doi.org/10.3390/nano11113056>
- Foroughi, F., Hassanzadeh-Tabrizi, S. A., & Amighian, J. (2015). Microemulsion synthesis and magnetic properties of hydroxyapatite-encapsulated nano CoFe<sub>2</sub>O<sub>4</sub>. *Journal of Magnetism and Magnetic Materials*, 382, 182–187. <https://doi.org/10.1016/j.jmmm.2015.01.075>
- Fortin, J.-P., Wilhelm, C., Servais, J., Ménager, C., Bacri, J.-C., & Gazeau, F. (2007). Size-Sorted Anionic Iron Oxide Nanomagnets as Colloidal Mediators for Magnetic Hyperthermia. *Journal of the American Chemical Society*, 129(9), 2628–2635. <https://doi.org/10.1021/ja067457e>
- Franco, A., Machado, F. L. A., & Zapf, V. S. (2011). Magnetic properties of nanoparticles of cobalt ferrite at high magnetic field. *Journal of Applied Physics*, 110(5), 053913. <https://doi.org/10.1063/1.3626931>
- Goldman, A. (2006). *Modern Ferrite Technology* (2nd ed.). Springer US.
- Gu, Z., Xiang, X., Fan, G., & Li, F. (2008). Facile Synthesis and Characterization of Cobalt Ferrite Nanocrystals via a Simple Reduction–Oxidation Route. *The Journal of Physical Chemistry C*, 112(47), 18459–18466. <https://doi.org/10.1021/jp806682q>
- Gul, I. H., & Maqsood, A. (2008). Structural, magnetic and electrical properties of cobalt ferrites prepared by the sol–gel route. *Journal of Alloys and Compounds*, 465(1–2), 227–231. <https://doi.org/10.1016/j.jallcom.2007.11.006>
- Gupta, A. K., & Gupta, M. (2005). Synthesis and surface engineering of iron oxide nanoparticles for biomedical applications. *Biomaterials*, 26(18), 3995–4021. <https://doi.org/10.1016/j.biomaterials.2004.10.012>
- H. Maeda, J. Wu, T. Sawa, Y. Matsumura, K. H. (2000). Tumor vascular permeability and the EPR effect in macromolecular therapeutics: a review. *Journal of Controlled Release*, 65, 271–284. [https://doi.org/S0168-3659\(99\)00248-5](https://doi.org/S0168-3659(99)00248-5)
- Houshiar, M., Zebhi, F., Razi, Z. J., Alidoust, A., & Askari, Z. (2014). Synthesis of cobalt ferrite (CoFe<sub>2</sub>O<sub>4</sub>) nanoparticles using combustion, coprecipitation, and precipitation methods: A comparison study of size, structural, and magnetic properties. *Journal of Magnetism and Magnetic Materials*, 371, 43–48. <https://doi.org/10.1016/j.jmmm.2014.06.059>
- Jun, Y., Huh, Y.-M., Choi, J., Lee, J.-H., Song, H.-T., Kim, S., Yoon, S., Kim, K.-S., Shin, J.-S., Suh, J.-S., & Cheon, J. (2005). Nanoscale Size Effect of Magnetic Nanocrystals and Their Utilization for Cancer Diagnosis via Magnetic Resonance Imaging. *Journal of the American Chemical Society*, 127(16), 5732–5733. <https://doi.org/10.1021/ja0422155>
- Khedr, M. H., Omar, A. A., & Abdel-Moaty, S. A. (2006). Magnetic nanocomposites: Preparation and characterization of Co-ferrite nanoparticles. *Colloids and Surfaces A: Physicochemical and Engineering Aspects*, 281(1–3), 8–14. <https://doi.org/10.1016/j.colsurfa.2006.02.005>
- M. R. Gauna, M. S. Conconi, S. Gomez, G. Suarez, E. F. Aglietti, N. M. R. (2015). Monoclinic - tetragonal zirconia quantification of commercial nanopowder mixtures by xrd and dta. *Ceramics – Silikáty*, 59(4), 318–325.
- Mathew, D. S., & Juang, R.-S. (2007). An overview of the structure and magnetism of spinel ferrite nanoparticles and their synthesis in microemulsions. *Chemical Engineering Journal*, 129(1–3), 51–65.

- <https://doi.org/10.1016/j.cej.2006.11.001>
- Méndez-Vilas, A. (2013). *Microbial Pathogens and Strategies for Combating Them: Science, Technology and Education*. Formatex Research Center.  
[https://books.google.com.bd/books/about/Microbial\\_Pathogens\\_and\\_Strategies\\_for\\_C.html?id=IHaYoAEA CAAJ&redir\\_esc=y](https://books.google.com.bd/books/about/Microbial_Pathogens_and_Strategies_for_C.html?id=IHaYoAEA CAAJ&redir_esc=y)
- Mohapatra, S., Rout, S. R., Maiti, S., Maiti, T. K., & Panda, A. B. (2011). Monodisperse mesoporous cobalt ferrite nanoparticles: synthesis and application in targeted delivery of antitumor drugs. *Journal of Materials Chemistry*, 21(25), 9185. <https://doi.org/10.1039/c1jm10732a>
- Patra, J. K., Das, G., Fraceto, L. F., Campos, E. V. R., Rodriguez-Torres, M. del P., Acosta-Torres, L. S., Diaz-Torres, L. A., Grillo, R., Swamy, M. K., Sharma, S., Habtemariam, S., & Shin, H.-S. (2018). Nano based drug delivery systems: recent developments and future prospects. *Journal of Nanobiotechnology*, 16(1), 71. <https://doi.org/10.1186/s12951-018-0392-8>
- Perez, J. M., Simeone, F. J., Tsourkas, A., Josephson, L., & Weissleder, R. (2004). Peroxidase Substrate Nanosensors for MR Imaging. *Nano Letters*, 4(1), 119–122. <https://doi.org/10.1021/nl034983k>
- Rietveld, H. M. (1969). A Profile Refinement Method for Nuclear and Magnetic Structures. *J. Appl. Cryst.*, 2, 65–71.
- Shafi, K. V. P. M., Gedanken, A., Prozorov, R., & Balogh, J. (1998). Sonochemical Preparation and Size-Dependent Properties of Nanostructured CoFe<sub>2</sub>O<sub>4</sub> Particles. *Chemistry of Materials*, 10(11), 3445–3450. <https://doi.org/10.1021/cm980182k>
- Sharrock, M. P. (1989). Particulate magnetic recording media: a review. *IEEE Transactions on Magnetics*, 25(6), 4374–4389. <https://doi.org/10.1109/20.45317>
- Sinkó, K., Manek, E., Meiszterics, A., Havancsák, K., Vainio, U., & Peterlik, H. (2012). Liquid-phase syntheses of cobalt ferrite nanoparticles. *Journal of Nanoparticle Research*, 14(6), 894. <https://doi.org/10.1007/s11051-012-0894-5>
- V. Pillai, D. O. S. (1996). Synthesis of high-coercivity cobalt ferrite particles using water-in-oil microemulsions. *Journal of Magnetism and Magnetic Material*, 163, 243–248.
- Verwey, E. J. W., & Heilmann, E. L. (1947). Physical Properties and Cation Arrangement of Oxides with Spinel Structures I. Cation Arrangement in Spinel. *The Journal of Chemical Physics*, 15(4), 174–180. <https://doi.org/10.1063/1.1746464>
- Wu, W., He, Q., & Jiang, C. (2008). Magnetic Iron Oxide Nanoparticles: Synthesis and Surface Functionalization Strategies. *Nanoscale Research Letters*, 3(11), 397. <https://doi.org/10.1007/s11671-008-9174-9>
- Yu, S., Gao, X., Baigude, H., Hai, X., Zhang, R., Gao, X., Shen, B., Li, Z., Tan, Z., & Su, H. (2015). Inorganic Nanovehicle for Potential Targeted Drug Delivery to Tumor Cells, Tumor Optical Imaging. *ACS Applied Materials & Interfaces*, 7(9), 5089–5096. <https://doi.org/10.1021/am507345j>
- Zeng, X., Zhang, J., Zhu, S., Deng, X., Ma, H., Zhang, J., Zhang, Q., Li, P., Xue, D., Mellors, N. J., Zhang, X., & Peng, Y. (2017). Direct observation of cation distributions of ideal inverse spinel CoFe<sub>2</sub>O<sub>4</sub> nanofibres and correlated magnetic properties. *Nanoscale*, 9(22), 7493–7500. <https://doi.org/10.1039/C7NR02013A>
- Zi, Z., Sun, Y., Zhu, X., Yang, Z., Dai, J., & Song, W. (2009). Synthesis and magnetic properties of CoFe<sub>2</sub>O<sub>4</sub> ferrite nanoparticles. *Journal of Magnetism and Magnetic Materials*, 321(9), 1251–1255. <https://doi.org/10.1016/j.jmmm.2008.11.004>